

## Nanoplasmonics for chemistry

Guillaume Baffou<sup>a</sup> and Romain Quidant<sup>\*bc</sup>

Cite this: *Chem. Soc. Rev.*, 2014, **43**, 3898

Received 15th October 2013

DOI: 10.1039/c3cs60364d

[www.rsc.org/csr](http://www.rsc.org/csr)

Noble metal nanoparticles supporting plasmonic resonances behave as efficient nanosources of light, heat and energetic electrons. Owing to these properties, they offer a unique playground to trigger chemical reactions on the nanoscale. In this tutorial review, we discuss how nanoplasmonics can benefit chemistry and review the most recent developments in this new and fast growing field of research.

### Key learning points

- Optical and thermal properties of noble metal nanoparticles.
- Generation of hot electrons in plasmonic nanoparticles.
- Mechanisms involved in plasmon-assisted chemistry.
- Application of plasmonic nanoparticles to different chemical reactions.

## Introduction

Over the last two decades, noble metal nanoparticles (NPs) have been the subject of extensive research in the frame of nanotechnology, mainly owing to their unique optical properties. Indeed, the free electron gas of such NPs features a resonant oscillation upon illumination in the visible part of the spectrum. The spectral properties of this resonance depend on the constitutive material, the geometry of the NP and its environment. This resonant electronic oscillation is called *localized surface plasmon* (LSP), and the field of research that studies the fundamentals and applications of LSP is known as *nanoplasmonics*.<sup>1</sup> LSPs are accompanied by valuable physical effects such as optical near-field enhancement, heat generation and excitation of hot-electrons. Hence, plasmonic NPs can behave as efficient nanosources of heat, light or energetic electrons, remotely controllable by light. In nanoplasmonics, these properties have stimulated extensive basic research and already led to a wide range of applications in nanotechnologies.

Light and heat are physical quantities involved in many mechanisms in physics, chemistry and biology. Hence, a natural

trend is to explore possible frameworks that could gain from the unique properties of metal NPs. So far, biology has been one of the areas of science that has benefited the most from nanoplasmonics. For instance, gold NPs as nanosources of heat are already at the basis of applications ranging from photothermal cancer therapy,<sup>2–4</sup> bio-imaging,<sup>5</sup> drug delivery<sup>6</sup> and nanosurgery.<sup>7</sup> Chemistry is another field of science that can potentially greatly profit from plasmonic NPs. Indeed, heat is a major parameter in any chemical reaction, light can be used to achieve high selectivity in chemical mechanisms thanks to quantum selection rules and adjustable photon energies, and electron transfer is the basis of redox reactions. Hence, the idea to use metal NPs as efficient nanosources of heat, light and electrons appears to be an appealing concept to both boost the yield of chemical reactions and improve their spatial and temporal control.

In this tutorial review, we survey recent advances in plasmon-assisted chemistry. The first section gives the readers the basics of nanoplasmonics. We successively describe the optical and thermal properties of metal NPs as well as the process of hot electron generation. In the second section we review the first class of studies in which the intense light field concentrated at the metal NP surface drives photochemical reactions. The third section focuses on exploiting the heat generated by metal NPs to control the yield of chemical reactions. Finally, the last section discusses how energetic electrons can be extracted from the NP to trigger chemical transformation of neighbouring reactants or enhance the efficiency of photocatalysts.

<sup>a</sup> CNRS, Aix Marseille université, Centrale Marseille, Institut Fresnel, UMR 7249, 13013 Marseille, France

<sup>b</sup> ICFO-Institut de Ciències Fotòniques, Mediterranean Technology Park, 08860 Castelldefels, Barcelona, Spain

<sup>c</sup> ICREA-Institució Catalana de Recerca i Estudis Avançats, 08010 Barcelona, Spain. E-mail: [romain.quidant@icfo.es](mailto:romain.quidant@icfo.es)

## Basics of nanoplasmonics

### Optical near field enhancement

Upon illumination, the free electron gas of a metal NP oscillates at the frequency of the incident electric field. This oscillation is further enhanced when the frequency of the incoming light matches its LSP resonance. Due to this electronic oscillation, the NP behaves as an electromagnetic dipole re-emitting light coherently at the same frequency. While part of this emitted light is scattered to the far field, the other is concentrated at the metal surface. Depending on the morphology of the NP, the enhancement of the optical near field can be gigantic. Fig. 1 presents numerical simulations, performed using the boundary element method (BEM),<sup>8,9</sup> of the optical near field around NPs of various geometries immersed in water while illuminated at their LSP resonance. As the result of the strong gradient of surface charges, optical intensity enhancements of several orders of magnitude are achieved either at the apex of tips, or by approaching two NPs very close together to form a nanometric insulating gap (55 for a sphere, 1800 for a dimer, 3000 for an ellipsoid and 33 000 for a dimer of ellipsoids). The dramatic increase of the available number of photons per unit volume at these optical “hot spots” is expected to increase the yield of photochemical reactions close to the surface of the metal. Some of the main developments based on this concept will be presented in the section Near-field assisted photochemistry.

### Heat generation

The resonant oscillation of the electronic gas of the NP is also responsible for energy dissipation into the metal *via* the Joule effect that results in heat generation and eventually an increase of the NP temperature.<sup>10</sup>

The total heat power  $P$  absorbed (and subsequently delivered to the environment) by a metal NP under continuous (cw) illumination can be directly estimated from its absorption cross-section  $\sigma_{\text{abs}}$ :

$$P = \sigma_{\text{abs}} I \quad (1)$$

where  $I$  is the light intensity (power per unit area). The associated temperature increase  $\delta T_{\text{NP}}$  does not only depend on  $P$ , but also on the NP morphology and the thermal conductivity of the surrounding medium. For a *spherical* NP in a uniform medium of thermal conductivity  $\kappa$ , there exists a simple analytical expression of  $\delta T_{\text{NP}}$ , which reads

$$\delta T_{\text{NP}} = P/(4\pi\kappa R) \quad (2)$$

where  $R$  is the radius of the NP. As an example, illuminating a 20 nm spherical gold NP in water ( $\kappa = 0.6 \text{ W m}^{-1} \text{ K}^{-1}$ ) with a green laser of 1 mW focused over  $1 \mu\text{m}^2$  leads to a temperature increase of  $\delta T_{\text{NP}} = 5 \text{ K}$ . The temperature profile outside the NP, in the surrounding medium, varies as  $1/r$  (where  $r$  is the radial coordinate, see Fig. 2a) according to:

$$\delta T(r) = P/(4\pi\kappa r) \quad (3)$$

It is important to notice that for *non-spherical* NPs, retrieving  $\delta T_{\text{NP}}$  from the knowledge of  $P$  is not straightforward, and numerical simulations are required.<sup>11,12</sup>

When using NPs, the heated region is so small that the thermal inertia of the system is very weak leading to a very fast heating and cooling dynamics. If  $L$  is the size of the heated region and  $D$  the thermal diffusivity of the surroundings, the time scale  $\tau$  governing the temperature dynamics of the system reads:

$$\tau = L^2/D \quad (4)$$

For instance, for  $L = 1 \mu\text{m}$  in water, temperature dynamics as fast as a few microseconds can be achieved. Such a fast dynamics, which is prohibited on the macroscopic scale, offers opportunities to achieve fast dynamic control of chemical reactions. Furthermore, an interesting consequence of this very fast dynamics is the further confinement of the temperature profile at the vicinity of the NP upon short pulse illumination. Fig. 2 illustrates this effect by comparing the spatial extension of the temperature profile around a spherical NP under cw and pulsed illumination. While a steady state temperature profile in



**Guillaume Baffou**

*Guillaume Baffou studied physics at the Ecole Normale Supérieure de Cachan and University Paris XI (France). He got his PhD in 2007 from the University Paris XI. He then spent 3 years at ICFO, the Institute of Photonic Science (Castelldefels, Spain), as a post-doc in the Plasmon Nanooptics group led by Prof. Romain Quidant. Since 2010, he has been a research scientist at the Institut Fresnel in Marseille, France. His research interests include plasmonics and associated thermal effects.*



**Romain Quidant**

*Romain Quidant received his PhD in Physics in 2002 from the University of Dijon (France). Since then he has worked in Barcelona at ICFO in the field of nanoplasmonics. In 2006, he was appointed junior Professor and a group leader of the Plasmon NanoOptics group at ICFO and became a tenure professor in 2009 both at ICFO and ICREA. His research focuses on the study of the optical properties of metal nano-structures and their use in the fabrication of future miniaturized optical functionalities and devices. Current activities include biosensing, quantum optics and optomechanics, optical manipulation and nanochemistry.*

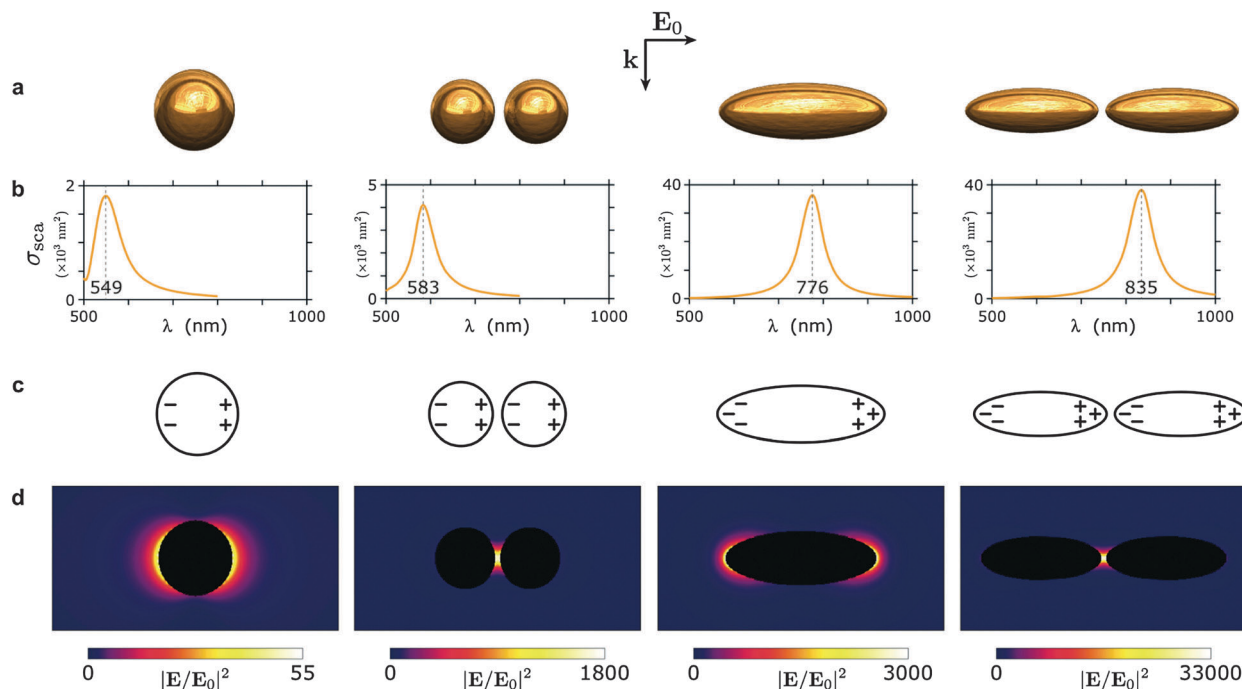


**Fig. 1** Influence of the NP geometry on the optical confinement and spectral features of the LSP resonance: (a) four geometries of gold NPs are considered: an isolated 50 nm sphere, a plasmonic dimer formed by two adjacent 40 nm NPs separated by 5 nm, an isolated oblate NP (100 nm long, aspect ratio of 3) and a dimer of oblate NPs (82 nm long, aspect ratio 3) separated by 5 nm. All four structures feature the same volume of gold. We consider an illumination from the top by a plane wave polarized horizontally. Sphere: 50 nm in diameter. (b) Simulations of the corresponding scattering cross sections showing the evolution of the LSP resonance (c) schematic of the charge distribution at a given time during the period of the charge oscillation. (d) Simulations of the distribution of the optical enhancement around the NPs at the respective LSP resonance wavelengths (simulations performed using the Boundary Element Method<sup>8,9</sup>).

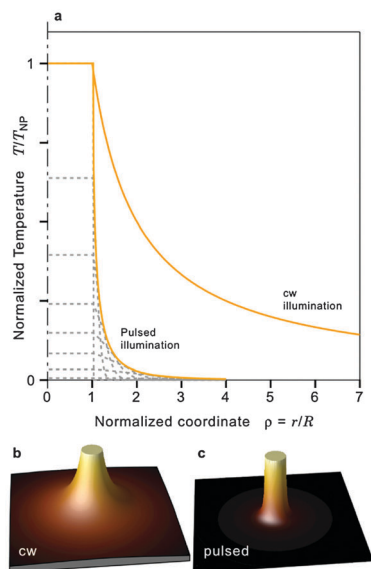


**Fig. 2** Temperature profile around a spherical gold nanoparticle for both cw and pulsed illuminations: (a) comparison of the temperature profiles under cw and pulsed illumination (dash line: temperature at different times after the pulse absorption). (b) and (c) Corresponding 3-D renderings. Reproduced with permission from ref. 13.

$1/r$  is observed under cw illumination, femtosecond-pulsed illumination leads to a much more confined profile in  $1/r^3$ .<sup>13</sup>

So far, the unique photothermal properties of plasmonic NPs have mostly benefited bio-related applications, such as cancer therapy, drug and gene delivery, photoacoustic imaging and nanosurgery.<sup>10</sup> Yet, since any area of science features thermal-induced processes, one can envision a broad applicability of this concept. Our focus of interest in the section Thermoplasmonics for chemistry is to show how this effect can be beneficial to chemical synthesis.

### Hot electron injection

Following the absorption of a photon, a free electron of the metal NP gets promoted to a higher energy level. This electronic transition will occur with a constant probability from below the Fermi level, creating a uniform probability to find the excited electron at energies between  $E_f$  and  $E_f + h\nu$ . Then, within a time scale of around 10 fs, this electron loses energy through electron–electron scattering, leading to a cascading process redistributing the energy of the primary electron to the electronic gas, creating a non-equilibrium Fermi–Dirac electron distribution. During this excitation and energy redistribution process, energetic electron transfer from the metal to nearby acceptors can occur *via* two different pathways. (1) A coherent process where the injected electron is the primary electron that absorbed a photon and did not interact with other electrons. (2) An incoherent process where the excited hot electron primarily undergoes electron–electron interaction.<sup>14</sup> In the latter case,

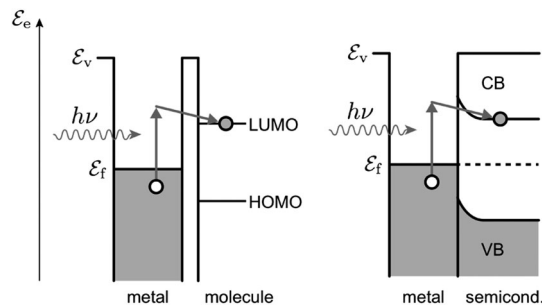


**Fig. 3** Hot electron transfer from a metallic NP to an adjacent electron acceptor: (left) electronic energy diagram of a metal nanoparticle at the vicinity of a molecule ( $E_f$  and  $E_v$  are the Fermi energy and the vacuum energy, respectively). Under illumination, a photo-excited electron is generated in the metal NP and tunnels to an unoccupied energy level in the molecule. (right) Electronic energy diagram of the junction between a metal and a semiconductor (Schottky junction). Under illumination, a photo-excited electron is generated in the metal NP and tunnels to the conduction band (CB) of the semiconductor.

the electron transfer relies on the interaction between the athermal Fermi–Dirac electron distribution with a nearby acceptor. In 2014, Govorov *et al.*<sup>15</sup> have theoretically shown that generation of hot electrons with large energies is favoured in small nanocrystals with sizes around 10–20 nm. Fig. 3 sketches the mechanisms of hot electron transfer for two different nearby reactants: a molecule and a semiconductor. In the first case, hot electrons from the NP can tunnel into the LUMO (lowest unoccupied molecular orbital) of an adsorbed molecular reactant located nearby the metal NP. In the second mechanism, the NP is in contact with a semiconductor. In this case, the equilibration of the Fermi level causes the bending of the conduction band of the semiconductor, and the possible formation of a Schottky barrier. Some recent studies based on this effect will be reviewed in the section Hot electron injection from plasmonic NPs.

### Overview of the main mechanisms in plasmon-assisted chemistry

The three processes described above, namely optical near-field enhancement, temperature increase and hot electron transfer,

can be involved in different mechanisms triggering chemical reactions. The six main mechanisms originating from these three elementary processes are listed in Fig. 4. In Mechanism A, a thermal-induced reaction is enhanced by the temperature increase around the plasmonic NP. In Mechanism B, the light concentration around the NP enhances the incident photon rate experienced by the nearby reactant. Mechanism C involves a hot electron created by photon absorption and transferred from the NP to an adjacent reactant. Another family of mechanisms involves a photocatalyst: the photocatalytic activity can be enhanced either by the NP temperature increase (Mechanism D) or the optical field enhancement at the catalyst location (Mechanism E). Finally, in Mechanism F, the catalyst is further activated by hot electron transfer from the plasmonic NP to the catalyst. Note that in the literature about plasmon-assisted chemistry, the identification of the involved mechanism(s) remains sometimes unclear (especially when using a photocatalyst), as discussed in the last section of this review.

## Near-field assisted photochemistry

In this section, we review recent advances in the use of plasmonic NPs to enhance the yield of photo-chemical processes. The capability of plasmonic nanostructures to enhance the light intensity at the metal surface enables both (i) to dramatically increase the efficiency of photochemical reactions by providing more photons per unit volume and (ii) to control these reactions in small volumes down to the nanometre scale. The idea of using a rough metallic surface to enhance the yield of surface reactions was first proposed by Nitzan and Brus<sup>16</sup> in 1981 and experimentally implemented two years later by Chen and Osgood.<sup>17</sup> In their pioneer experiment, the authors demonstrated enhanced UV photo-dissociation of organometallic molecules at the surface of UV resonant cadmium nanoparticles. Following this proof of concept, many different experiments have been reported in the literature. Hereafter we classify the main contributions into four categories.

In the first family of experiments, NPs were used to control photo-polymerization on the nanometre scale. In this approach

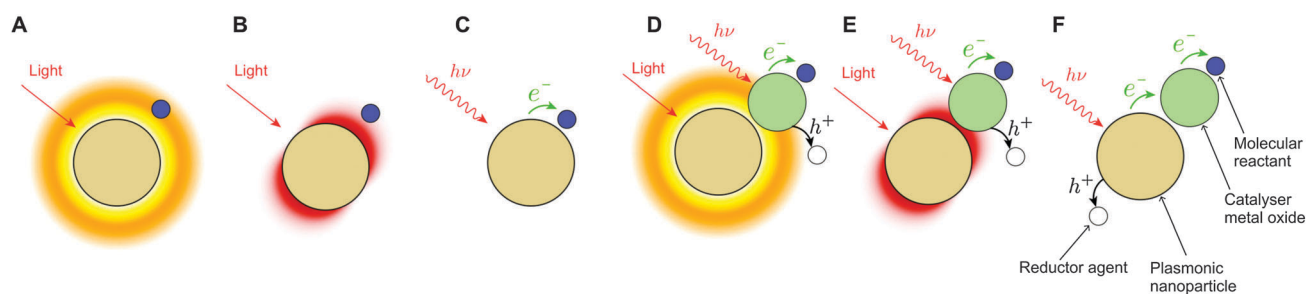


**Fig. 4** Main physical mechanisms involved in plasmon-assisted chemistry: Mechanism A: the photo-induced temperature increase of the NP provides heat to an adjacent reactant. Mechanism B: the enhancement of the optical near field at the vicinity of the NP increases the photon rate seen by an adjacent reactant. Mechanism C: a photo-induced hot electron is transferred to a nearby reactant. Mechanism D: the electron–hole ( $e^-$ – $h^+$ ) generation rate in a photocatalyzer is enhanced by heat generated by the NP. Mechanism E: the electron–hole generation rate in a photocatalyzer is enhanced by the strong optical near-field of the plasmonic NP. Mechanism F: the photocatalyst adjacent to the NP is activated by hot electron transfer from the plasmonic NP.

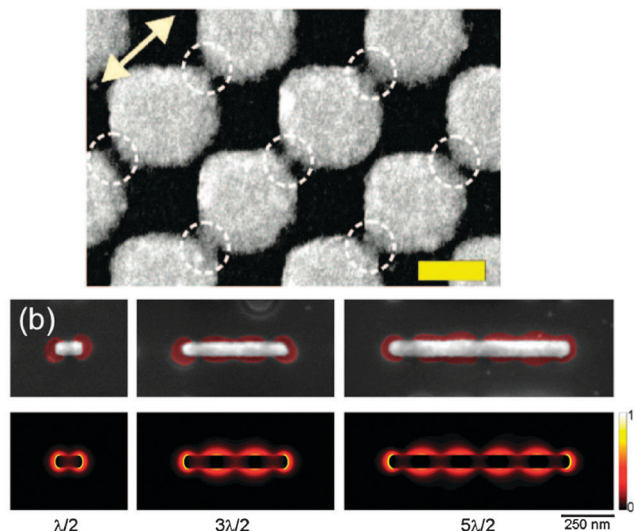


**Fig. 5** (a) Nanoscale photopolymerization of SU8: the SEM image of an array of closely packed gold NPs after 3 h exposure with a cw source polarized linearly along the direction indicated by the arrow. The dashed circles highlight the polymerized regions (scale bar = 100 nm). Reprinted with permission from ref. 18 (Copyright 2008 American Chemical Society). (b) Four-photon absorption lithography in PMMA enables us to map successive odd resonant modes in gold nanorods: (top) SEM images with exposed PMMA (highlighted in red) around  $\lambda/2$ -,  $3\lambda/2$ -, and  $5\lambda/2$ -antennas. All antennas are resonant at 860 nm. For the three exposures, the incident power on the antennas is 4, 31, and 103  $\mu\text{W}$ , respectively. (bottom) Normalized electric near-field intensities computed in the half-plane of the different rods. Reprinted with permission from ref. 19 (Copyright 2012 American Chemical Society).

a pattern of plasmonic nanostructures is covered with a thin layer of polymers. The degree of photo-polymerization is contrasted according to the non-uniform optical field intensity surrounding the NPs. Hence, imaging the regions where polymerization occurs makes it possible to map the optical near-field of NPs. In 2008, Ueno *et al.*<sup>18</sup> used a SU8 polymer layer deposited on a pattern of lithographic gold nanostructures and they observed the local polymerization in the hot spot regions induced by a two-photon absorption (Fig. 5). Besides its interest to map the near field around plasmonic structures, this experiment is conceptually important since it demonstrates that chemical reactions induced by two-photon absorption can be initiated even under cw illumination. This may enable cost- and energy-effective nanolithography, microscopy, as well as exploitation of nonlinear absorption in solar energy conversion.

In 2012, Volpe *et al.*<sup>19</sup> employed the opposite strategy that consists in optically breaking PMMA polymer chains on the nanoscale. The exposed regions can be specifically dissolved forming holes in the polymer layer. This mechanism is quite similar to e-beam lithography where the PMMA chains get broken by accelerated electrons instead of photons. In practice PMMA has an absorption peak in the UV range of the spectrum (centred at 213 nm) but is transparent to visible or infrared light where plasmonic nanostructures resonate. To compensate for this wavelength mismatch, the authors rely on the absorption of four near infrared (NIR) photons. The high brightness of

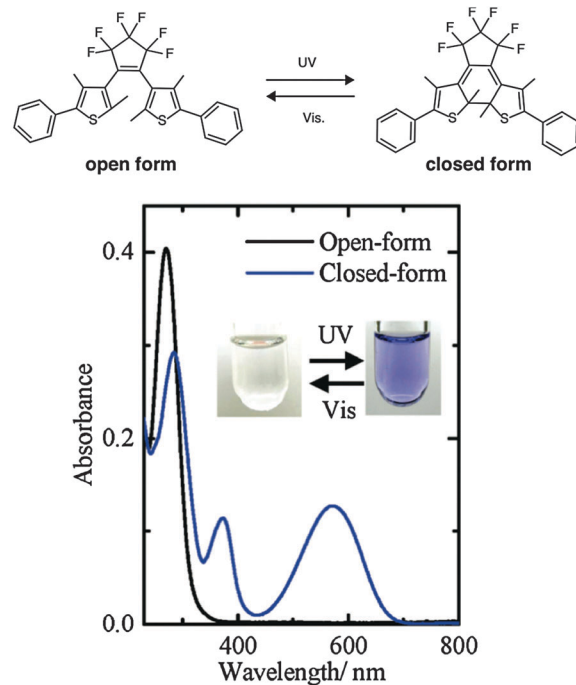


**Fig. 6** Isomer structures of a diarylethene molecule along with the absorption spectra. Reprinted with permission from ref. 20 (Copyright 2009 American Chemical Society).

resonant plasmonic nanoparticles provides high enough intensity to boost this otherwise very inefficient mechanism. This work enabled the mapping of the optical near field of various plasmonic modes in gold nanostructures with an unprecedented spatial resolution.

The third family of experiments focuses on isomerisation, which is the re-arrangement of the atoms of a molecule. Isomerisation is certainly the easiest way to illustrate the concept of plasmon-induced photochemistry as it involves only one reactant and one product and many isomerizations can be photo-induced. The most classical example is the photo-isomerization of diarylethene (DE) molecules. Tsuboi *et al.*<sup>20</sup> evidenced in 2009 the ring opening of DE molecules in solution assisted by cw NIR illumination of gold NPs at  $\lambda = 800$  nm (Fig. 6). Since this excitation wavelength  $\lambda$  did not match the absorption of the molecule, two-photon absorption was proposed as the involved mechanism. This assumption was corroborated by a quadratic dependence of the reaction yield as a function of the laser power. This work is another illustration of the ability of plasmonic NPs to trigger non-linear processes even under moderate cw illumination. It is worth mentioning a direct application of plasmonic-assisted photo-isomerisation to high-resolution optical lithography. Azobenzene (AB) molecules are known to undergo *trans-cis* isomerisation under photo-excitation with visible light. When grafted to PMMA, the use of polarized light enables molecular rotation through thermal diffusion within the PMMA matrix. AB molecules thus play the role of molecular motors, pushing or pulling the polymeric host as reorientation occurs. This results in a mass transport from high to low local intensity regions that provide a very

high-resolution snapshot of the illumination field. When combined with plasmonics, it becomes possible to control photo-isomerisation on the true nanometre scale as only the AB molecules at the vicinity of the hot spots will undergo an isomerisation. This one step rearrangement of the polymer topography has applications in photo-lithography as it enables nanoscale resolution with visible light and it results to be another simple and powerful way to map with a nanoscale resolution the near field optical response of plasmonic nanoscale systems.<sup>21–23</sup>

Another promising concept proposed in 2012 consists in imprinting with nanometre accuracy a specific chemical functional group at predefined locations of metallic nanostructures. The non-uniform distribution of the optical near field intensity bound to the nanostructure controls the site and the extent of the photochemical reaction at the metal surface. A first illustration of this concept relies on cleaving the nitroveratryloxy carbonyl (NVOC) group of an organosilane upon pulsed NIR illumination.<sup>24</sup> The absorption of two NIR photons by the NVOC group (absorption maximum of around 350 nm) leads to the formation of free amine groups at the gold surface where the plasmonic field is more intense, *i.e.* at the tips of the crescent nanostructures. After exposure, the sample was incubated with COOH functionalized gold colloids to create an amide bond between the amines at the exposed regions and the carboxylic groups at the surface of the gold nanoparticles. Scanning Electron Microscopy (SEM) indicates that the gold colloids preferentially bind to the crescent tips. Another implementation of this concept relies on the so-called Light Assisted Molecular Immobilization (LAMI).<sup>25–27</sup> LAMI exploits an inherent natural property of proteins and peptides whereby a disulfide bridge is disrupted upon absorption of UV photons by the nearby aromatic amino acids. The created free thiol groups are subsequently used to immobilize the protein or the peptide to a thiol-reactive substrate. In 2013, Galloway *et al.*<sup>28</sup> used a plasmonics approach to achieve protein immobilization with nanometre accuracy in the nanogap between two adjacent gold nanoparticles. The immobilized protein was subsequently used as a scaffold to attach a single gold nanocolloid (Fig. 7). This universal technique is envisioned to benefit a wide range of applications and more especially biochemical sensing and enhanced spectroscopy whose performance strongly depends on the relative position of the analyte and the optical hot spot.

## Photothermal chemistry

The rate  $K$  of most chemical reactions follows the Arrhenius law

$$K(T) = A \exp(-E_a/RT) \quad (5)$$

where  $T$  is the temperature of the reaction medium,  $A$  a constant,  $E_a$  the activation energy and  $R$  the ideal gas constant. According to this law,  $K$  increases with the temperature  $T$ . By exploiting the capability of plasmonic NPs to efficiently heat upon illumination, one can locally control the yield of chemical reactions.

While using plasmonic NPs as enhanced nanosources of light in photochemistry is an idea that was born in 1981,<sup>16</sup>

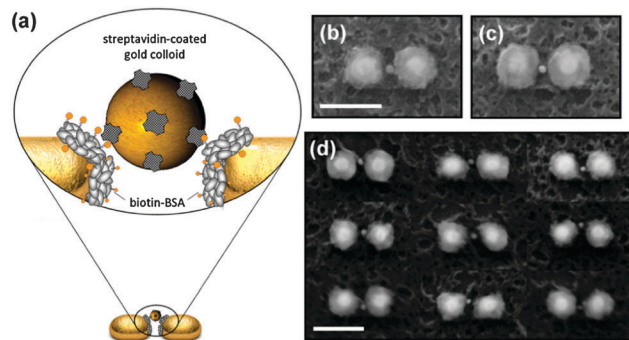


Fig. 7 Light assisted molecular immobilization in the gap of gold dimers: (a) schematic of the chemical modification used to bind a gold colloid to the immobilized protein. (b and c) SEM images showing binding of a single gold nanoparticle in the gap of homogeneous gold dimers. (d) Series of SEM images that illustrates self-alignment of the gold colloid in the hot spot despite the morphological irregularities of the hosting dimers (scale bar = 150 nm). Reprinted with permission from ref. 28 (Copyright 2013 American Chemical Society).

surprisingly, their use as enhanced nanosources of heat to control the yield of chemical reactions is much more recent as its first implementation dates from 2007.<sup>29</sup> Several factors could explain this delay. On the one hand, *thermoplasmonics* is a very recent field of research that was born in 2002 within a medical frame.<sup>30,31</sup> Before this date, heat generation by plasmonic NPs was mostly considered as a side effect. On the other hand, it took some time to identify what heating by plasmonic NPs could further provide beyond conventional macroscopic heating using a hot plate. Hereafter are listed the main advantages of using metal NPs as nanosources of heat:

- Reducing the heated region makes it possible to improve the heating dynamics due to a reduced thermal inertia of the system.
- Heating a micrometric area makes it possible to achieve solvent superheating (above the boiling point) under ambient pressure conditions, which would otherwise require the use of a bulky apparatus, such as an autoclave.<sup>32</sup>
- Finally, like in near-field assisted photochemistry, heating based on the illumination of metallic NPs could make it possible to control a chemical reaction down to the nanometre scale, thus enabling the formation of products at a specific location.

In 2007, Cao *et al.*<sup>29</sup> reported on the first illustration of the potential of thermoplasmonics in chemistry. The authors reported on the plasmon-assisted growth of semiconductor nanowires by flowing a precursor gas ( $\text{SiH}_4$  or  $\text{GeH}_4$ ) over gold NPs shined with a cw laser. Growth of nanowires is known to occur at temperature above 380 °C. Here, such temperature could be achieved without macroscopic heating by simply illuminating a gold NP pattern with 20 mW during less than one minute. This approach enabled the authors to control the growth of single nanowires at predefined locations of the patterned surface. In 2009, Yen and El-Sayed<sup>33,34</sup> reported on the reduction of a cyanoferrate complex assisted by gold NP illumination. While several possible mechanisms were considered, the

authors concluded that the chemical transformation was solely induced by heating of the entire reaction medium. This conclusion is somehow disappointing since it means that similar results would have been obtained using a hot plate; none of the advantages listed above was here evidenced. Adleman *et al.*<sup>35</sup> reported on plasmon-assisted catalysis (PAC). The authors induced the formation of a gas phase (bubbles) in a liquid reaction medium by illuminating gold NPs lying on the substrate. For a liquid environment composed of a mixture of water and ethanol, the authors evidenced the formation of H<sub>2</sub>, CO and CO<sub>2</sub> molecules coming from the reforming of ethanol. The work illustrates the fact that gold NPs can act as catalysts that can be activated when heated up upon illumination.

In 2008, Chen *et al.*<sup>36</sup> evidenced the synergistic effect of a mixture of gold NPs and metal oxide powders for the oxidation of volatile organic compounds such as formaldehyde (HCHO) into CO<sub>2</sub>. The authors explained the enhancement of the photocatalytic activity by a plasmonic increase of the catalyst temperature (Fig. 4, Mechanism D). The authors also evoked the interaction between the local electromagnetic field and the dipolar moment of the molecules as a possible additional effect responsible for the reported observations.

In 2010, Hung *et al.*<sup>37</sup> studied the cooperative effect of plasmonic gold NPs and metal oxides (Fe<sub>2</sub>O<sub>3</sub>) on the reaction rate of the oxidation of carbon monoxide CO to carbon dioxide CO<sub>2</sub>. Their data show that metal oxide acts a photocatalyst whose efficiency is enhanced by the heat delivered by the NPs. Remarkably, their data underline that the plasmon driven catalytic reaction rate was several orders of magnitude higher than the one obtained under conventional uniform heating. In several reported studies, NP heating is often not the only effect responsible for the enhanced reaction yield. More complex mechanisms sensitive to heating but involving transient electron transfer have been proposed,<sup>38</sup> as detailed in the next section.

## Hot electron injection from plasmonic NPs

Heterogeneous catalysis is of critical importance in chemical, environmental and energy conversion processes. Among catalytic mechanisms, photocatalysis aims at converting photons into electricity or fuels, or to degrade chemical waste and pollutants. Ideally, such photoconversion processes would be triggered by clean and inextinguishable sunlight. So far, however, most photocatalytic systems have been operated with UV illumination and show low efficiency in the visible range, limiting thus the use of solar energy. In this context, plasmonic NPs have recently raised great promise.<sup>39–41</sup> In 2003, it was evidenced that the presence of noble metal NPs could increase the efficiency of neighbouring photocatalysts *via* a hot electron injection mechanism.<sup>42</sup> Since then, this approach has been applied to a large variety of catalytic reactions, such as water splitting, hydrogen splitting, CO<sub>2</sub> reduction to organic compounds or molecular degradation.<sup>43</sup> In the following, we review a selection of important contributions to this field.

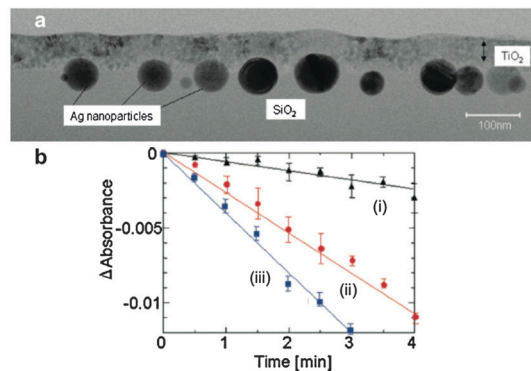
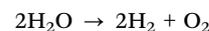


Fig. 8 Plasmon-assisted decomposition of methylene blue using an Ag–TiO<sub>2</sub> system: (a) TEM view of the cross section of a TiO<sub>2</sub> film deposited on silver NPs lying on a SiO<sub>2</sub> substrate. (b) Decomposition rate of methylene blue as a function of time. (i) A TiO<sub>2</sub> film on a SiO<sub>2</sub> substrate. (ii) A TiO<sub>2</sub> film on a Ag–SiO<sub>2</sub> core–shell structure on a SiO<sub>2</sub> substrate. SiO<sub>2</sub> thickness of (i) and (ii) was 20 nm. (iii) A TiO<sub>2</sub> film on a Ag–SiO<sub>2</sub> core–shell structure where SiO<sub>2</sub> thickness was 5 nm on a SiO<sub>2</sub> substrate. Reprinted with permission from ref. 46 (Copyright 2008 American Chemical Society).

In a pioneer communication in 2004, Tian and Tatsuma<sup>44</sup> studied for the first time a system composed of nanoporous TiO<sub>2</sub> and gold NPs upon visible illumination, as a potential improved photocatalyst based on photo-induced electron transfer from the NPs to TiO<sub>2</sub> (Fig. 4, Mechanism F). A few months later, the same authors reported the experimental evidence of their prediction by demonstrating the catalytic oxidation of methanol and ethanol by oxygen.<sup>45</sup>

In 2008, Awazu *et al.*<sup>46</sup> reported on a similar experiment in which they examined the decomposition of dye molecules (methylene blue) on Ag–SiO<sub>2</sub> core–shell NPs coated with a thin TiO<sub>2</sub> layer (Fig. 8). The chemical yield was enhanced seven folds by the presence of the Ag NPs. However, a different mechanism was proposed to explain the enhanced catalytic activity of the TiO<sub>2</sub>. The authors concluded that the enhanced optical field experienced by TiO<sub>2</sub> leads to a higher rate in the electron–hole generation (Mechanism E). In 2010, Christopher, Ingram and Linic<sup>47</sup> re-examined this experiment with the aim of unravelling the actual involved mechanism. Various plasmonic NP materials and geometries were investigated. They ended up with the same mechanism originally proposed by Awazu and evidenced a strong influence of the NP shape and size on the photocatalytic activity (Fig. 9): while gold NPs feature a low activity due to the mismatch between the plasmonic resonance of the Au NP and the absorption band of TiO<sub>2</sub>, silver nano-cubes featured the best catalytic enhancement.

Several studies have recently demonstrated that plasmonic photocatalysis can also dramatically improve the yield of the water splitting reaction, which is one of the most attractive reactions in the quest for clean energy.



Efficient and cost effective water splitting would be a key technology towards the so-called *hydrogen economy* in which

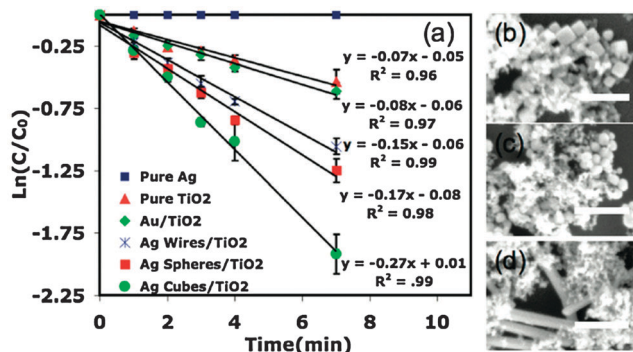


Fig. 9 Influence of the structural parameters of the plasmonic NPs on plasmon-assisted decomposition of methylene blue: (a) evolution of reactant concentration (methylene blue molecules) as a function of time for different catalytic systems. The highest photocatalytic activity was observed for silver nanocubes. (b–d) SEM micrographs of Ag nanocubes/TiO<sub>2</sub> composites (b), Ag nanospheres/TiO<sub>2</sub> composites (c), Ag nanowires/TiO<sub>2</sub> composites (d). Reproduced with permission from ref. 47 (Copyright 2010 American Chemical Society).

hydrogen would be used as a clean source for most of our energy needs. It is also worth mentioning that water splitting is also the initial step of photosynthesis; hence mastering it would contribute to the development of *synthetic photosynthesis* for the generation of chemical energy through the synthesis of carbohydrates and sugars. In practice plasmon-assisted water splitting can be achieved by decorating TiO<sub>2</sub> powder with metallic NPs.<sup>48</sup> In certain circumstances, silver was shown to be more efficient than gold due to better matching of its LSPR resonance with the semiconductor absorption spectrum.<sup>49</sup> In the 2013, the Moskovits' group reported on plasmon-enhanced solar water splitting using a carpet of gold nanorods (Fig. 10).<sup>50</sup> Vertically orientated gold nanorods were grown by electrodeposition in a porous anodic aluminium oxide template. The nanorods were first coated with a thin TiO<sub>2</sub> layer for charge separation. TiO<sub>2</sub> was then covered by tiny Pt NPs, which trigger the reduction of hydrogen ions, after capturing the hot electrons. Finally, a cobalt based catalyst was used to feed the metal back with electrons. The fabricated composite shows enhanced responsivity across the plasmon band of the gold nanorods. Furthermore, the system features long operational stability with no decrease in activity over tens of hours of solar illumination.

In 2011, Christopher *et al.*<sup>38</sup> proposed an alternative strategy in which metal NPs illuminated at their plasmonic resonance can play the role of photocatalysts by themselves, without metal oxides. The authors evidenced the oxidation of molecules such as ethylene, CO and NH<sub>3</sub> solely by illuminating silver NPs. The proposed mechanism is based on the generation of hot electrons and their direct transfer to adsorbed O<sub>2</sub> molecules to form O<sub>2</sub><sup>-</sup> radicals that facilitate the O<sub>2</sub> dissociation and the associated oxidation of the molecules of interest. In this study, standard macroscopic heating of the sample at around 450 K was required to induce the reaction. The illumination contributed to increase the yield by a factor of 4. The question was raised whether the illumination was not just further heating the sample by optical absorption, since a rise of the sample temperature by

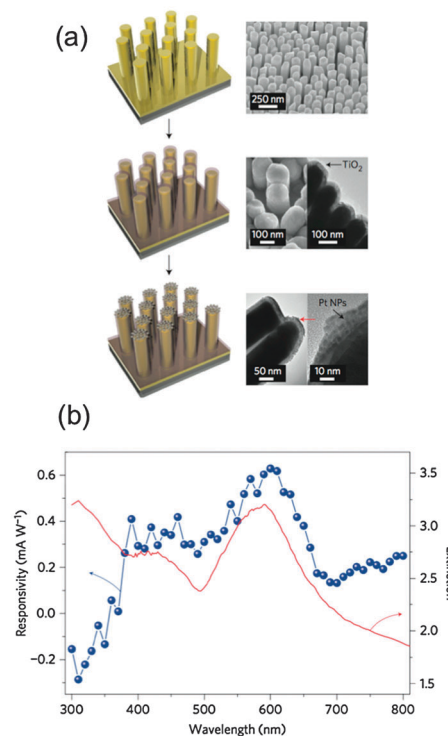


Fig. 10 Plasmon-assisted water splitting: (a) description of the plasmonic photocathode used in ref. 50. (b) Evolution of the measured photocurrent as a function of the wavelength of the incident light. The response matches the extinction spectrum of the device (red line). Reprinted with permission from ref. 50.

solely 21 K would give exactly the same enhancement factor. The question was addressed but the insignificance of photo-thermal effects was not convincingly established at this stage. The same group published in 2012 a follow-up work where they explained how the linear dependence of the reaction rate as a function of the laser power turns into a super-linear dependence at relatively low intensity if the NPs are re-arranged in a close packed manner.<sup>51</sup> This observation tends to demonstrate the dominant role of transient electron transfer in the underlying mechanism to the detriment of a photo-thermal process. This work was intended to demonstrate that plasmonic NPs stand for valuable alternatives to commonly used metal oxides as efficient photocatalyzers. It also illustrates how hard it usually is to discriminate among different possible involved mechanisms.

Nearly at the same time, Halas' group reported the H<sub>2</sub> dissociation on gold NPs.<sup>52</sup> Dissociation of H<sub>2</sub> is one of the most important but also one of the most challenging reactions in heterogeneous catalysis. Indeed, the energy of the H<sub>2</sub> bond is too high (4.5 eV) to cleave the H<sub>2</sub> molecules by thermal heating. So far H<sub>2</sub> dissociation has been performed at the surface of metals, using very strong oxidants or upon very strong laser fields. In this experiment, the sample consisted of small gold NPs in a TiO<sub>2</sub> matrix. According to the authors, here TiO<sub>2</sub> does not act as an electron donor as in previously reported studies but aims at retaining H<sub>2</sub> a sufficiently long time near the gold surface. Interestingly, no temperature increase seems to be required in this approach, which differs

from the observation of Christopher *et al.* using silver NPs for water splitting.<sup>51</sup> The main difference here is that H<sub>2</sub> splitting is not a redox reaction as the redox potential of the hydrogen atoms is not modified. Hence, the process is not limited by the Fermi energy of the metal, which lies below the potential of the reduction half-reaction.<sup>43</sup>

## Concluding remarks

In this tutorial we present the foundations and review the main advances in the fast growing field of plasmonic nanochemistry. Owing to their unique interaction with light, metallic NPs can contribute to boost the yield of chemical reactions through different mechanisms, involving photons, heat or energetic electrons. While studies have demonstrated great potential of the thematic, plasmon-assisted chemistry is only at its infancy. At the research level, lots of efforts are currently put into exploring other aspects of chemistry that could benefit from metallic NPs. From a more applied perspective, the applicability of this concept to industrial synthesis still needs to be assessed and demonstrated.

## Acknowledgements

This work was partially supported by the European Community's Seventh Framework Program under grant ERC-Plasmolight (no. 259196) and Fundació privada CELLEX.

## Notes and references

- S. Lal, S. E. Clare and N. J. Halas, *Acc. Chem. Res.*, 2008, **41**, 1842.
- P. Cherukuri, E. S. Glazer and S. A. Curley, *Adv. Drug Delivery Rev.*, 2010, **62**, 339–345.
- X. Huang, P. K. Jain, I. H. El-Sayed and M. A. El-Sayed, *Laser Med. Sci.*, 2008, **23**, 217–228.
- L. Cognet, S. Berciaud, D. Lasne and B. Lounis, *Anal. Chem.*, 2008, **80**, 2288–2294.
- B. T. Timko, T. Dvir and D. S. Kohane, *Adv. Mater.*, 2010, **22**, 4925.
- A. Urban, T. Pfeiffer, M. Fedoruk, A. Lutich and J. Feldmann, *ACS Nano*, 2011, **5**, 3585–3590.
- M. Pelton, J. Aizpurua and G. Bryant, *Laser Photonics Rev.*, 2008, **2**, 136–159.
- F. J. Garcia de Abajo and A. Howie, *Phys. Rev. B: Condens. Matter Mater. Phys.*, 2002, **65**, 115418.
- U. Hohenester and A. Trügler, *Comput. Phys. Commun.*, 2012, **183**, 370–381.
- G. Baffou and R. Quidant, *Laser Photonics Rev.*, 2013, **7**, 171.
- G. Baffou, R. Quidant and C. Girard, *Phys. Rev. B: Condens. Matter Mater. Phys.*, 2010, **82**, 165424.
- G. Baffou, R. Quidant and F. J. Garcia de Abajo, *ACS Nano*, 2010, **4**, 709.
- G. Baffou and H. Rigneault, *Phys. Rev. B: Condens. Matter Mater. Phys.*, 2011, **84**, 035415.
- M. J. Kale, T. Avanesian and P. Christopher, *ACS Catal.*, 2014, **4**, 116–128.
- A. O. Govorov, H. Zhang and Y. K. Gun'ko, *J. Phys. Chem. C*, 2013, **117**, 16616–16631.
- A. Nitzan and L. E. Brus, *J. Chem. Phys.*, 1981, **75**, 2205.
- C. J. Chen and R. M. Osgood, *Phys. Rev. Lett.*, 1983, **50**, 1705.
- K. Ueno, S. Juodkakis, T. Shibuya, Y. Yokota, V. Mizeikis, K. Sasaki and H. Misawa, *J. Am. Chem. Soc.*, 2008, **130**, 6928–6929.
- G. Volpe, M. Noack, S. S. Acimović, C. Reinhardt and R. Quidant, *Nano Lett.*, 2012, **12**, 4864–4868.
- Y. Tsuboi, R. Shimizu, T. Shoji and N. Kitamura, *J. Am. Chem. Soc.*, 2009, **131**, 12623–12627.
- S. Davya and M. Spajer, *Appl. Phys. Lett.*, 1986, **69**, 3306.
- F. H'dhili, R. Bachelot, G. Lerondel, D. Barchiesi and P. Royer, *Appl. Phys. Lett.*, 2001, **79**, 4019.
- C. Hubert, *et al.*, *Nano Lett.*, 2005, **5**, 615–619.
- K. H. Dostert, M. Álvarez, K. Koynov, A. del Campo, H. J. Butt and M. Kreiter, *Langmuir*, 2012, **28**, 3699.
- T. Snabe, G. A. Roder, M. T. Neves-Petersen, S. Buusb and S. B. Petersen, *Biosens. Bioelectron.*, 2006, **21**, 1553–1559.
- M. T. Neves-Petersen, T. Snabe, S. Klitgaard, M. Duroux and S. P. Petersen, *Protein Sci.*, 2006, **15**, 343–351.
- M. Duroux, E. Skovsen, M. T. Neves-Petersen, L. Duroux, L. Gurevich and S. B. Petersen, *Proteomics*, 2006, **7**, 3491.
- C. M. Galloway, M. P. Kreuzer, S. S. Acimović, G. Volpe, M. Correia, S. B. Petersen, M. T. Neves-Petersen and R. Quidant, *Nano Lett.*, 2013, **13**, 4299.
- L. Cao, D. N. Barsic, A. R. Guichard and M. L. Brongersma, *Nano Lett.*, 2007, **7**, 3523.
- C. M. Pitsillides, E. K. Joe, X. Wei, R. R. Anderson and C. P. Lin, *Biophys. J.*, 2003, **84**, 4023–4032.
- D. Boyer, P. Tamarat, A. Maali, B. Lounis and M. Orrit, *Science*, 2002, **297**, 1160.
- G. Baffou, J. Polleux, R. Rigneault and S. Monneret, *J. Phys. Chem. C*, 2014, DOI: 10.1021/jp411519k.
- C. W. Yen and M. A. El-Sayed, *J. Phys. Chem. C*, 2009, **113**, 19585–19590.
- M. A. El-Sayed, *J. Photochem. Photobiol., A*, 2011, **221**, 138–142.
- J. R. Adleman, D. A. Boyd, D. G. Goodwin and D. Psaltis, *Nano Lett.*, 2009, **9**, 4417–4423.
- X. Chen, H. Y. Zhu, J. C. Zhao, Z. F. Zheng and X. P. Gao, *Angew. Chem., Int. Ed.*, 2008, **47**, 5353–5356.
- W. H. Hung, M. Aykol, D. Valley, W. Hou and S. B. Cronin, *Nano Lett.*, 2010, **10**, 1314–1318.
- P. Christopher, H. Xin and S. Linic, *Nat. Chem.*, 2011, **3**, 467.
- P. Weng, B. Huang, Y. Dai and M. H. Whangbo, *Phys. Chem. Chem. Phys.*, 2012, **14**, 9813.
- X. Zhang, Y. Lim Chen, R. S. Liu and D. Ping Tsai, *Rep. Prog. Phys.*, 2013, **76**, 046401.
- M. Xiao, R. Jiang, F. Wang, C. Fang, J. Wang and J. C. Yu, *J. Mater. Chem. A*, 2013, **1**, 5790.
- D. N. Denzler, C. Frischkorn, C. Hess, M. Wolf and G. Ertl, *Phys. Rev. Lett.*, 2003, **91**, 226102.
- W. Hou and S. B. Cronin, *Adv. Funct. Mater.*, 2013, **23**, 1612–1619.

- 44 Y. Tian and T. Tatsuma, *Chem. Commun.*, 2004, 1810.
- 45 Y. Tian and T. Tatsuma, *J. Am. Chem. Soc.*, 2005, **127**, 7632.
- 46 K. Awazu, *et al.*, *J. Am. Chem. Soc.*, 2008, **130**, 1676.
- 47 P. Christopher, D. B. Ingram and S. Linic, *J. Phys. Chem. C*, 2010, **114**, 9173–9177.
- 48 A. Primo, T. Marino, A. Corma, R. Molinari and H. García, *J. Am. Chem. Soc.*, 2011, **133**, 6930.
- 49 D. B. Ingram and S. Linic, *J. Am. Chem. Soc.*, 2011, **133**, 5202–5205.
- 50 S. Mubeen, J. Lee, N. Singh, S. Krämer, G. D. Stucky and M. Moskovits, *Nat. Nanotechnol.*, 2013, **8**, 247.
- 51 P. Christopher, H. Xin, A. Marimuthu and S. Linic, *Nat. Mater.*, 2012, **11**, 1044.
- 52 S. Mukherjee, *et al.*, *Nano Lett.*, 2013, **13**, 240–247.